THE JOURNAL OF PHYSICAL CHEMISTRY A
A JOURNAL OF THE AMERICAN CHEMICAL SOCIETY

pubs.acs.org/JPCA Article

Photochemistry of Hypervalent Iodoazide Derivatives

Published as part of The Journal of Physical Chemistry A special issue "Massimo Olivucci Festschrift".

Nikita Gupta, Haoran Zhu, Joseph M. O'Shea, Anoklase jean-Luc Ayitou, Russell J. Hemley, Tom G. Driver, and Ksenija D. Glusac*

Cite This: https://doi.org/10.1021/acs.jpca.5c02567 Read Online

ACCESS | Metrics & More | Article Recommendations | Supporting Information

ABSTRACT: The photochemical properties and reaction mechanisms of a series of hypervalent iodoazide compounds ($R-IN_3$) were investigated, with substituents ($-CH_3$, $-H$, $-CF_3$) tuning the electronic density of the phenyl ring. With the help of UV irradiation, ultrafast time-resolved spectroscopy, and density functional theory (DFT) calculations, we elucidated the mechanisms of azide radical ($N_3^\bullet$) release and its subsequent reactivity. UV−vis spectroscopy reveals that the photoconversion rates follow the trend $CH_3 > H > CF_3$, aligning with DFT-calculated ΔG values for ring-opening transitions. Homolytic cleavage of the I−N bond is identified as the dominant pathway for $N_3^\bullet$ generation upon UV irradiation, occurring within 400 fs. The released azide radicals react with the solvent molecules, while the iodo radical $R-I_C^\bullet$ fragments undergo a thermodynamically uphill lactone ring-opening (RO) reaction and subsequent hydrogen atom abstraction from the solvent to form carboxylic acids R−I−COOH, as validated by NMR and IR spectroscopy. The study also highlights the role of substituents in influencing reaction kinetics and intermediate stability, with electron-donating groups accelerating the release of the $N_3^\bullet$ species. This work bridges experimental observations with computational predictions, offering a foundation for future advancements in azide-based reactions and materials.

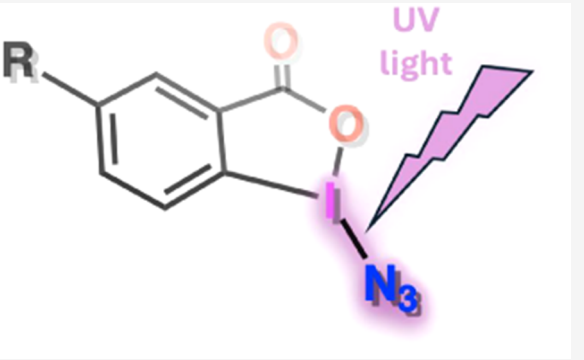

INTRODUCTION

Organic azides exhibit remarkable chemical reactivity, driven by their unique amphiphilic nature that enables the reactions with electrophiles at the N1 position and nucleophiles at the N3 position, as well as by the ease of N−N bond cleavage.[1−3] For example, the nucleophilic attack at the N1 position of azides using different reducing agents, such as phosphines utilized in the Staudinger reaction, represents an efficient method to synthesize organic amines.[4] An electrophilic attack at the N3 position plays a key role in the Schmidt and Curtius rearrangements, where the azide anion undergoes a nucleophilic attack on carbonyl groups. These reactions are widely utilized for the synthesis of amine and amide derivatives.[5] Azides are also 1,3-dipoles, participating readily in [2 + 3] cycloaddition reactions, such as the well-known "click chemistry" reaction, where an azide reacts with an alkyne to form 1,2,3-triazoles.[6] The click cycloaddition[7] has opened vast opportunities for forming carbon−nitrogen and nitrogen-heteroatom bonds and constructing functional group libraries.[3,8−11] Finally, thermal activation or photolysis of organic azides releases molecular nitrogen, generating highly reactive nitrenes.[12,13] The nitrenes can insert into C−H bonds, enabling C−H amination, or react with C═C bonds to facilitate alkene aziridination.[14] At low temperatures, nitrenes can undergo intersystem crossing to a triplet ground state, which can dimerize to generate azocompounds.[15]

These versatile reactions have made azides indispensable tools in synthetic chemistry, facilitating the creation of diverse molecular libraries for a wide range of biological applications. In drug discovery, they enable the synthesis of nitrogen-containing bioactive compounds,[16] while in bioconjugation, they are integral to click chemistry, providing a mild and efficient method to link functional groups—such as fluorescent probes—to biological systems.[17] Azides are also used in polymer chemistry, where nitrene or click chemistry is used in azide-containing polymers to cross-link the chains and enhance material performance in applications including ion-conducting membranes, solar cells, light-emitting diodes, self-healing materials, and others.[2,18]

The Zhdankin reagent, shown as compound $H-IN_3$ in Scheme 1, is an iodine(III) compound commonly used to synthesize organic azides under mild conditions and with good

Received: April 15, 2025
Revised: June 5, 2025
Accepted: June 6, 2025

Scheme 1. Model Compounds Investigated in This Study

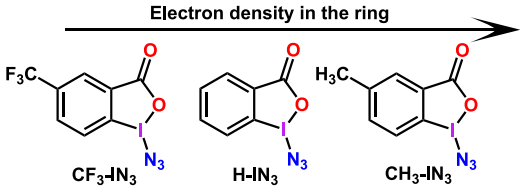

functional group tolerance.[19−23] The reactivity of H−IN_3 is associated with the presence of nonclassical "hypervalent" O−I−N_3 bonds formed from each lobe of a single 5p orbital of iodine.[24−27] As a result, O−I−N_3 bonds contain only three electrons and are quite weak; the I−N bond dissociation energy of H−IN_3 is estimated computationally to be only 35.4 kcal/mol.[28] Thermal and photochemical I−N bond homolysis in H−IN_3 has been demonstrated as an efficient method to form azide radicals needed for the formation of organic azides.[29−44] Due to the presence of labile azide groups, H−IN_3 is an explosive chemical that exhibits a heat of release of 1770 kJ/kg and a TD_{24} of 45 °C (TD_{24} is the temperature at which the maximum decomposition rate occurs over 24 h).[32] The use of H−IN_3 in synthesis has prompted researchers to investigate other cyclic analogs, and these studies have shown that lactone-based derivatives exhibit reduced explosivity while maintaining good azide transfer reactivity.[32]

In the present study, we investigate a series of hypervalent iodo-azide compounds (R−IN_3) to ascertain the photorelease dynamics and kinetics of azide radicals and their subsequent reactions, focusing on how the electronic nature of the ring influences the "deazidation" processes. Employing spectroscopic and computational methods, we identified homolytic dissociation of the iodo-azide bond upon UV irradiation as the primary pathway leading to the formation of $N_3^{\bullet}$ species within 400 ps. The dissociation rate is strongly modulated by the electron density in the phenyl ring, with electron-rich substituents accelerating the process. Crucially, the overall reaction rate is determined by the lactone ring-opening, during which the iodine-centered radical intermediate transitions to the oxygen-centered radical, highlighting the importance of electronic effects in controlling this key transformation. Subsequently, the azide radical abstracts a hydrogen atom from the solvent, yielding benzoic acid as the final product, confirmed through NMR and IR spectroscopy. Notable shifts in energy dynamics, influenced by ring substituents, underscore the critical role of electronic effects in bond dissociation and subsequent reaction pathways. These findings provide mechanistic insights into the photochemistry of iodoazides, emphasizing the influence of electronic substituents on reaction kinetics and pathways.

RESULTS AND DISCUSSION

The compounds CH_3−IN_3, H−IN_3, and CF_3−IN_3 were synthesized following established protocols and characterized using ^{1}H NMR spectroscopy (Figure S1). The methoxy derivative (MeO−IN_3) was also synthesized, but due to its high light sensitivity, further characterization was not possible. The electronic transitions in model azides were evaluated using a combination of experimental UV−vis absorption spectroscopy and computational time-dependent density functional theory (Figure 1). The experimental spectra for all three compounds appear below 350 nm and consist of an intense band at ∼230 nm and a weaker absorption feature with a peak

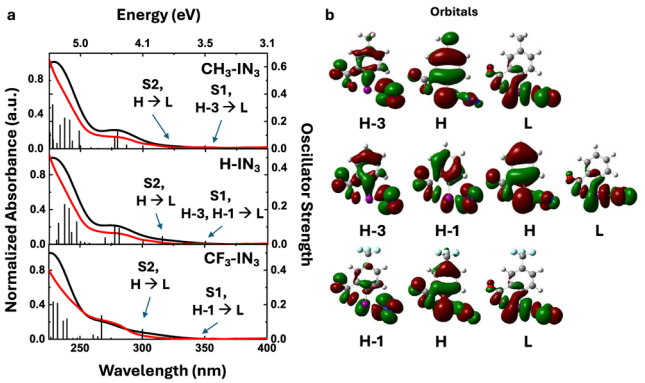

Figure 1. (a) Comparison of the calculated (black curves) and experimental (red) UV−vis spectra for the three compounds (experiments were performed in acetonitrile solutions). Vertical lines indicate calculated electronic transitions at the MN15/cc-pVTZ/SSD level of theory with the IEFPCM solvation model for solvation effects. (b) Molecular orbitals depict the charge distribution in the relevant electronic states.

at ∼280 nm. The effect of the phenyl substituent on the absorption spectra is minor, and only a modest red shift of peak maxima is observed with increasing electron-donating ability of the substituents. The computational analysis was performed using the MN15 functional, which has been recognized previously for its broad accuracy.[45] The calculated UV−vis absorption spectra are qualitatively consistent with the experimental values, as shown in Figure 1. The orbitals associated with the lowest energy transitions are shown in Figure 1 and were used to assign the relevant transitions. The S_1 and S_2 transitions in all three compounds involve charge accumulation in LUMOs, which are delocalized over azide-iodo-lactone moieties. The occupied orbitals involved in the transitions (HOMO, HOMO−1, and HOMO−3) are generally delocalized over the entire π-framework of the compounds, indicating that the S_1 and S_2 transitions exhibit charge transfer character, where electronic density is pushed from the phenyl ring to the azide-iodo-lactone moiety. The only exception to this assignment is the S_1 state of CF_3−IN_3, where the HOMO−3 orbital is mostly confined to the azide-iodo-lactone ring, likely due to the electron-withdrawing character of the $-CF_3$ group. Overall, the population of the S_1 state in all model compounds is expected to lead to charge density accumulation at the azide group.

To investigate the photochemical activity of iodoazides, UV-irradiation experiments were conducted on argon-purged azide solutions using a 275 nm excitation source. The photochemical changes were monitored using UV−vis spectroscopy, as shown in Figure 2. All three model compounds exhibited photochemical activity, as witnessed by the temporal changes in their UV−vis spectra. Spectra for the corresponding benzoic acid and acetate, as plausible products, were also collected to match with the components for all three samples shown in Figure 2. Given that the spectra for the corresponding benzoic acid and acetate have very similar UV−vis spectra, it is inconclusive to establish the nature and structure of the products formed from UV−vis absorption studies. The kinetics of the UV-irradiation experiments were derived from the absorption data in Figure 2 using a sequential 1→2→3 model (shown in Figure 3). The lifetimes τ_1, associated with the 1→2 transition appear in the 500−800 s range, while the subsequent 2→3 transitions occur with lifetimes in the 1000−5000 s range. Interestingly, the

https://doi.org/10.1021/acs.jpca.5c02567
J. Phys. Chem. A XXXX, XXX, XXX−XXX

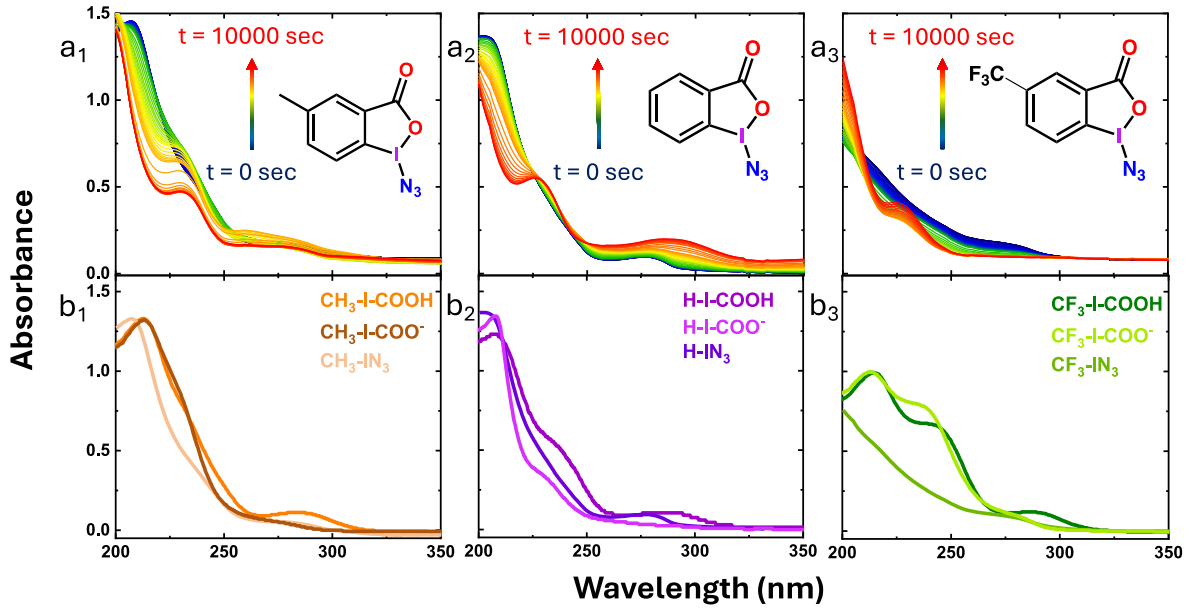

Figure 2. UV irradiation of R−IN_3 samples monitored by UV−vis spectroscopy in acetonitrile under an inert atmosphere (Ar). (a1−a3) Time-resolved UV−vis spectral changes observed for CH_3−IN_3, H−IN_3, and CF_3−IN_3 upon UV light irradiation. (b1−b3) Experimental UV−vis spectra of R−IN_3 and their corresponding R−I−COOH and R−I−COONa products.

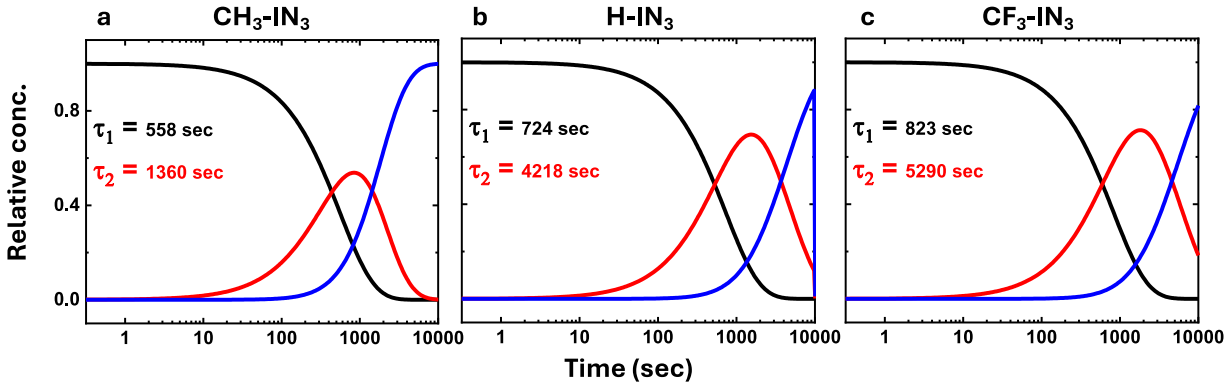

Figure 3. Time-dependent concentration profiles of the components involved in the photochemical transformation of (a) CH_3−IN_3, (b) H−IN_3, and (c) CF_3−IN_3 derived from UV irradiation experiments and analyzed by using principal component analysis. The black, red, blue, and green curves represent Components 1, 2, and 3, respectively.

photoconversion is seemingly faster for derivatives with electron-donating substituents than for electron-withdrawing synthons, with CH_3 > H > CF_3 in rate constants for both processes.

The formation of H−I−COOH from H−IN_3 under irradiation was confirmed by using ^{1}H NMR spectroscopy. The reaction was monitored over time in an argon-purged J-Young NMR tube with dry DMSO-d_6 as the solvent, and the results are shown in Figure 4. The spectra clearly illustrate the conversion of H−IN_3 to H−I−COOH, with distinct changes observed in the chemical shifts. Notably, a characteristic signal at 7.5 and 7.2 ppm, corresponding to the carboxylic acid group, emerged, while the signal at 7.8 ppm, associated with the initial iodoazide (H−IN_3) progressively diminished (see Figure S1 for NMR peaks of H−IN_3). A similar transition was observed for CF_3−IN_3 to CF_3−I−COOH (see Figure S3). These results provide direct evidence of the photochemical transformation of R−IN_3 to R−I−COOH.

Infrared (IR) spectroscopy provided additional insights into the reactivity of H−IN_3. Upon UV irradiation, distinct spectral changes occurred in the azide and carbonyl regions, as shown in Figure 5. The starting H−IN_3 solution exhibited an

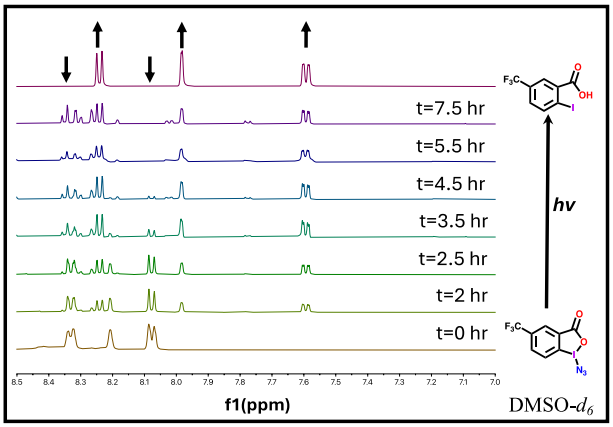

Figure 4. UV irradiation of H−IN_3 in DMSO-d_6, monitored using ^{1}H NMR in a J. Young NMR tube under an argon atmosphere.

https://doi.org/10.1021/acs.jpca.5c02567
J. Phys. Chem. A XXXX, XXX, XXX−XXX

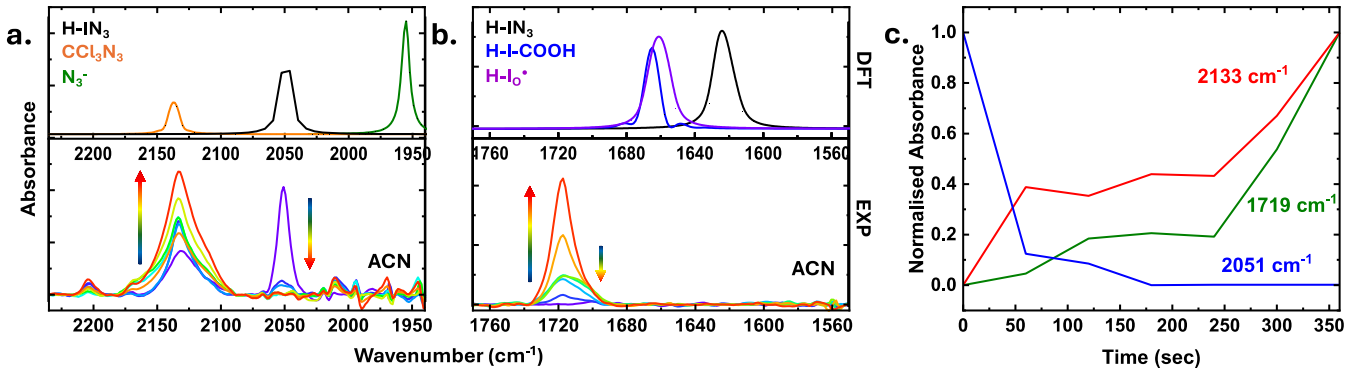

Figure 5. (a, b) DFT-calculated IR spectra (MN15 functional and cc-pVTZ/SDD basis set with IEFPCM = acetonitrile as the solvation method) are shown in the top panel, while changes in experimentally collected IR spectra of H−IN_3 recorded on irradiation with a UV lamp under an argon atmosphere (in CCl_4) are shown in the bottom panel. (c) Evolution of the IR peak at red: 2133 cm^{-1}, green: 1719 cm^{-1}, and blue: 2051 cm^{-1} with time on UV irradiation under an argon atmosphere.

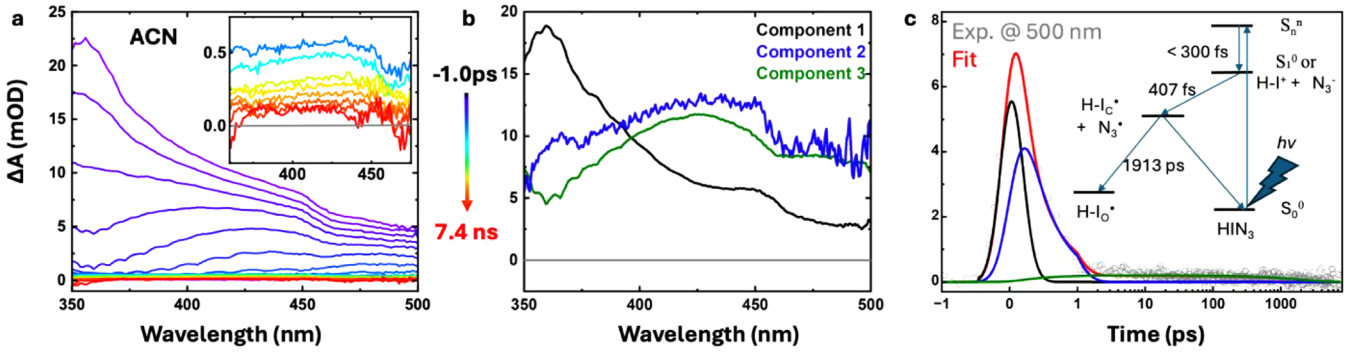

Figure 6. Femtosecond transient absorption spectra for H−IN_3. (a) Spectral trace for H−IN_3 (ex = 295 nm) in ACN, under Ar. Transient spectra were collected in time intervals ranging from 0 to 7400 ps. The inset shows spectral traces at later times. (b) Component profiles obtained from global analysis fitting, highlighting the transitions between species. (c) Kinetic traces for H−IN_3 monitored at 500 nm. Solid red lines show fits for the sequential kinetic model. Black, blue, and green represent the populations of the first, second, and third components used for data fitting.

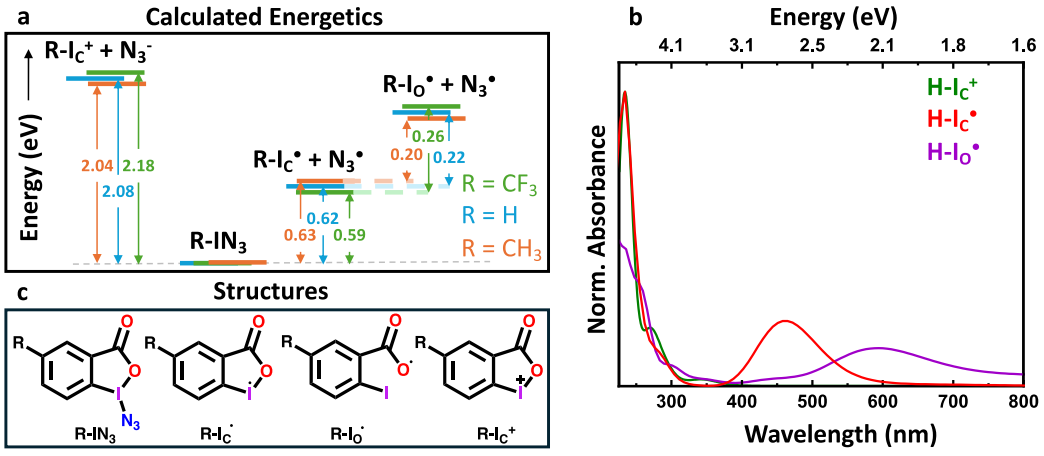

Figure 7. (a) Energetics for homolytic and heterolytic dissociation of R−IN_3 obtained using the computational method with the MN15 functional and cc-pVTZ/SDD basis set with IEFPCM = acetonitrile as the solvation method. (b) Calculated absorption spectra of H−$I_C^{\bullet}$, H−$I_O^{\bullet}$, and H−I_C^{+}. (c) Structures of the possible dissociation products.

absorption band at 2050 cm^{-1} that matches well with the density functional theory (DFT)-calculated stretching frequency of the azide group at 2049 cm^{-1} (Figure S4).[46,47] This peak disappeared within the first few minutes of irradiation, and a slower growth of a new peak emerged at 2133 cm^{-1}. The IR spectra of the possible photoproducts were calculated at the MN15/cc-pVTZ/SSD level of theory with IEFPCM solvation model for solvation effects, and the results are shown in Figure S5 and Table S1. The products of homolytic and heterolytic I−N bond scission, N_3^- and $N_3^{\bullet}$, have IR bands at 1810 cm^{-1} and 1443 cm^{-1} and do not match the experimentally observed peak at 2148 cm^{-1}. However, the experimentally observed peak matches well with the calculated azide stretching frequency of CCl_3N_3, indicating that homolytic I−N bond scission is likely followed by a reaction of photogenerated radicals with carbon tetrachloride, the solvent used in these experiments.[48,49] The

https://doi.org/10.1021/acs.jpca.5c02567
J. Phys. Chem. A XXXX, XXX, XXX−XXX

Table 1. DFT-Calculated Gibbs Free Energies for Ring Opening (RO) and Hydrogen Atom Abstraction (HAA) Reactions[a]

	Homolytic Reaction	$-CH_3$	$-H$	$-CF_3$
ΔG_{RO}	$R-I_C^{\bullet} \rightarrow R-I_O^{\bullet}$	0.20	0.22	0.26
ΔG_{HAA_O}	$R-I_O^{\bullet} + S-H \rightarrow R-I-COOH + S^{\bullet}$	−0.63	−0.65	−0.73
ΔG_{HAA_C}	$R-I_C^{\bullet} + S-H \rightarrow R-I-COOH + S^{\bullet}$	−0.43	−0.43	−0.47

[a]HAA involves acetonitrile (labeled as S−H) as an H-atom donor, and the calculations were performed from open (ΔG_{HAA_O}) and closed (ΔG_{HAA_C}) radical intermediates. Energies are reported in eV.

changes in the carbonyl stretching region are shown in Figure 5, where a peak shift and increased intensity were observed from 1707 to 1717 cm^{-1}. These changes are consistent with the calculated C═O stretching frequencies of $H-IN_3$ and H−I−COOH, further confirming that carboxylic acid is formed in the photochemical reaction of these organic azides. The kinetics of azide dissociation, shown in Figure 5, reveals that cleavage occurs within a few seconds of UV irradiation. At the same time, the growth of product bands is delayed, indicating the involvement of at least one intermediate (X) between $H-IN_3$ and H−I−COOH. Intermediate X was not observed in the IR window.

To elucidate the early photodissociation kinetics, we performed femtosecond transient absorption (fsTA) spectroscopy on argon-purged solutions of $H-IN_3$ (Figure 6). The transient spectrum obtained immediately after the photoexcitation pulse exhibits a broad excited-state absorption spanning 300−600 nm, with a maximum at 350 nm. This species decays within a few hundred femtoseconds, leaving a weak transient signal centered at 425 nm that persists on the time scale of our instrument (7.4 ns). The transient absorption data were analyzed using a 3-component model, as shown in Figure 6. The decay components were characterized by lifetimes of τ_1 < 300 fs (instrument response function) and τ_2 = 407 fs, as shown in Figure 6. Component 1, with rapid decay, is attributed to ultrafast electronic relaxation processes, such as internal conversion (IC) from the hot state (S_n^n) to the relaxed excited state (S_0^1) or potentially prompt heterolytic I−N bond cleavage, while acknowledging that its exact nature cannot be definitively determined due to the temporal limitations of our measurements.[50] The longer-lived component 2, with a 407 fs lifetime, is assigned to the formation of the organic radical $R-I_C^{\bullet}$, formed upon I−N photolysis (the structure of $R-I_C^{\bullet}$ is shown in Figure 7). This assignment is supported by DFT calculations discussed below. The kinetics of the 500 nm intermediate were further monitored, showing that the intermediate exhibits a 1913 ps lifetime.

DFT calculations were conducted to evaluate the thermodynamics of possible reaction pathways, as shown in Figure 7. We considered two pathways: one involving the homolytic I−N scission to form neutral radicals $R-I_C^{\bullet}$ and $N_3^{\bullet}$ and another associated with the heterolytic bond scission to form ionic species $R-I_C^{+}$ and N_3^{-}. The calculated Gibbs free energies show that the homolytic dissociations are significantly less thermodynamically demanding (ΔG values are in the 0.59−0.63 eV range) than the corresponding heterolytic pathways (ΔG values are in the 2.00−2.20 eV range). While both heterolytic and homolytic pathways are accessible from the molecular S1 excited states (whose energies are in the 3.5−4 eV range, Figure 1), we anticipate that the homolytic scission producing radicals $R-I_C^{\bullet}$ and $N_3^{\bullet}$ is the thermodynamic sink for both pathways. Thus, it is very likely that the photochemical reactivity of organic azides studied here generates radicals $R-I_C^{\bullet}$ and $N_3^{\bullet}$.

Interestingly, the substituent effects, though subtle, are different for the two pathways: the homolytic pathway is less energetically demanding for CF_3-substituted derivatives, while the heterolytic pathway favors electron-donating CH_3 substituents. In general, the stability and reactivity of the resulting radicals are governed by their electrophilic or nucleophilic nature.[51−53] Electrophilic radicals preferentially undergo reduction to form stabilized anions, while nucleophilic radicals are more readily oxidized to yield cations.[53,54] The trends observed in our calculations for the homolytic pathway suggest that the $R-I_C^{\bullet}$ radicals exhibit nucleophilic character (Figure 7).

Since benzoic acid derivatives were observed as reaction products in the NMR experiments (Figure 4), we further evaluated the energetics of RO from closed $R-I_C^{\bullet}$ to open $R-I_O^{\bullet}$ species, followed by H-atom abstraction from the solvent to form the corresponding benzoic acids (Figure 7). The RO reactions are slightly thermodynamically uphill, with the calculated ΔG values in the 0.20−0.26 eV range. This range is accessible at room temperature (as discussed later), enabling the formation of the RO radical intermediate, $R-I_O^{\bullet}$, as a relevant species in the reaction pathway. The substituent trend observed in the RO reactions indicates that electron-donating substituents favor the RO pathway (the calculated ΔG value for the CH_3 substituted derivative is only 0.20 eV). This behavior is because electron-donating groups stabilize the radical intermediate formed in the RO process by increasing electron density at the radical center.[52] The thermodynamically uphill RO process is also consistent with the long-lived 500 nm intermediate observed in the fsTA experiments shown in Figure 6. These experiments showed that the 500 nm intermediate is formed within 407 fs and persists for 1913 ps. To assign this intermediate, we evaluated the absorption spectra of $H-I_C^{\bullet}$, $H-I_O^{\bullet}$, and $H-I_C^{+}$ (Figure 7). We find that $H-I_C^{\bullet}$ absorbs in the 400−600 nm range, supporting our assignment of the 500 nm intermediate in the TA data to this species.

The substituent effects observed in the reaction kinetics in Figures 2 and 3 indicate that electron-donating substituents accelerate the overall photoreaction. This trend is consistent with the DFT-calculated ΔG_{RO} values for the RO in Figure 7 and Table 1 ($R-I_C^{\bullet} \rightarrow R-I_O^{\bullet}$), which predict that electron-withdrawing substituents are less energetically demanding. Thus, the overall reaction is likely not controlled by the rate of I−N bond homolysis. Instead, we propose that the formation of intermediate $R-I_O^{\bullet}$ controls the overall reaction, followed by hydrogen-atom abstraction (HAA_O), with the solvent serving as the H-atom donor. To support this conclusion, we calculated the free energies for the HAA from acetonitrile (labeled as solvent S−H) for both open ($R-I_O^{\bullet}$) and closed ($R-I_C^{\bullet}$) radicals, ΔG_{HAA_O} and ΔG_{HAA_C} (Table 1 and Figure S6). The trends observed in our experiment (CH_3 substituted azide reacts faster) are consistent with the calculated trends for the RO reactions and not the subsequent HAA processes,

https://doi.org/10.1021/acs.jpca.5c02567
J. Phys. Chem. A XXXX, XXX, XXX−XXX

Scheme 2. Proposed Mechanism for the Photodissociation of R−IN$_3$ Compounds

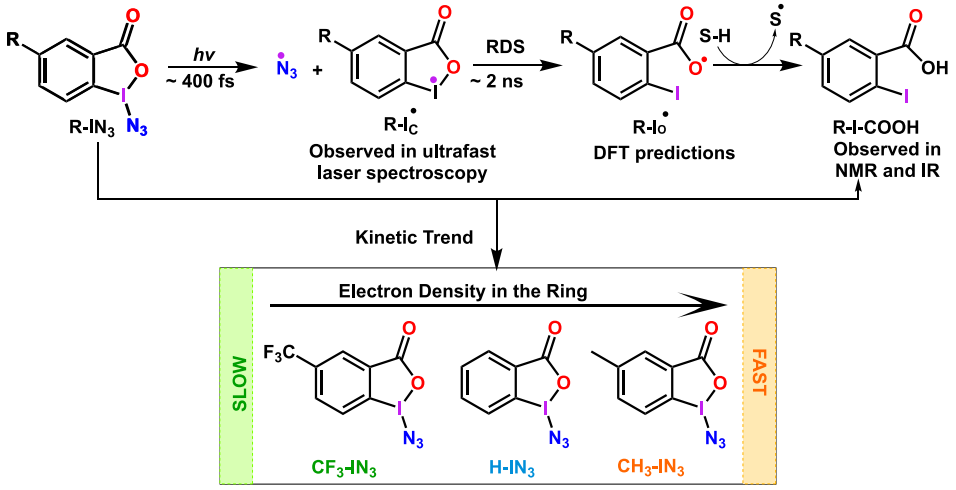

supporting our assignment of the RO reaction as the rate-determining step.

Based on the results shown above, we propose a reaction mechanism (Scheme 2) that starts with the UV excitation of R−IN$_3$ to induce transitions from S_0^0 to a vibrationally and electronically excited state S_n^n. The subsequent ultrafast subfemtosecond process is attributed to the internal conversion to the S_1 state (S_1^0), from which homolytic I−N bond cleavage takes place. Alternatively, prompt heterolytic cleavage may initially generate R−I$^+$ and N_3^-, followed by electron transfer from N_3^- to R−I$^+$. Both the process ultimately lead to homolytic I−N bond cleavage products to form $N_3^\bullet$ the cyclic radical intermediate R−I$_C^\bullet$. The rate constant for the RO of H−I$_C^\bullet$ to H−I$_O^\bullet$ can be estimated from time-resolved data in Figure 6, using the fits of the kinetic profile for the 400−500 nm intermediate assigned to H−I$_C^\bullet$. The rate constant for this decay was determined to be 3.6×10^8 s^{-1}. If we assume that RO is barrierless, then the DFT-calculated ΔG_{RO} = 0.22 eV (Table 1) can be used in an Arrhenius equation to derive an estimate for the RO rate constant. We find that the rate constant of 3.6×10^8 s^{-1} is obtained at room temperature when the pre-exponential factor $A = 1.8 \times 10^{12}$ is used. Such a pre-exponential factor is reasonable and consistent with typical iodo radical reactions,[55−57] supporting our assignment of the 3.6×10^8 s^{-1} process to the H−I$_C^\bullet$ → H−I$_O^\bullet$ ring-opening reaction. The final step involves abstraction of hydrogen from the solvent, yielding R−I−COOH. We hypothesize that the overall rate of conversion is governed by the RO step (H−I$_C^\bullet$ → H−I$_O^\bullet$), with the free energy barrier (ΔG_{RO}) increasing as electron density on the phenyl ring decreases, following the trend CF$_3$ > H > CH$_3$. These findings highlight the intricate interplay of electronic effects and mechanistic pathways in the photochemical reactivity of iodoazides.

CONCLUSION

In conclusion, this study investigates the photochemical behavior of hypervalent iodide compounds (R−IN$_3$) with varying electronic properties by modifying the R group (−CH$_3$, −H, and −CF$_3$). All compounds exhibit photochemical activity, with reaction rates following the trend CH$_3$ > H > CF$_3$, consistent with DFT-calculated ΔG_{RO} values that predict the energy demand for intermediate formation during RO. The photochemical transformation of R−IN$_3$ to R−I−COOH is confirmed through NMR and IR spectroscopy, with IR further indicating that the released azide radical reacts with the solvent. Homolytic dissociation of the I−N bond is identified as the primary pathway for azide radical ($N_3^\bullet$) release, occurring within a few hundred femtoseconds, as revealed by ultrafast transient absorption spectroscopy. The electronic properties of substituents significantly influence reaction kinetics, with electron-donating groups facilitating faster radical release. These findings advance our understanding of azide photochemistry and provide a foundation for designing efficient, stable, and safe energetic and functional materials.

ASSOCIATED CONTENT

Supporting Information

The Supporting Information is available free of charge at https://pubs.acs.org/doi/10.1021/acs.jpca.5c02567.

Material synthesis and characterization, experimental details for TA measurements, and computational details (PDF)

AUTHOR INFORMATION

Corresponding Author

Ksenija D. Glusac − *Department of Chemistry, University of Illinois Chicago, Chicago, Illinois 60607, United States; Chemical Sciences and Engineering, Argonne National Laboratory, Lemont, Illinois 60439, United States;* orcid.org/0000-0002-2734-057X; Email: glusac@uic.edu

Authors

Nikita Gupta − *Department of Chemistry, University of Illinois Chicago, Chicago, Illinois 60607, United States; Chemical Sciences and Engineering, Argonne National Laboratory, Lemont, Illinois 60439, United States*

Haoran Zhu − *Department of Chemistry, University of Illinois Chicago, Chicago, Illinois 60607, United States*

Joseph M. O'Shea − *Department of Chemistry, University of Illinois Chicago, Chicago, Illinois 60607, United States*

Anoklase jean-Luc Ayitou − *Department of Chemistry, University of Illinois Chicago, Chicago, Illinois 60607, United States;* orcid.org/0000-0001-6355-2564

https://doi.org/10.1021/acs.jpca.5c02567
J. Phys. Chem. A XXXX, XXX, XXX−XXX

Russell J. Hemley − *Department of Chemistry, University of Illinois Chicago, Chicago, Illinois 60607, United States; Department of Physics and Department of Earth and Environmental Sciences, University of Illinois Chicago, Chicago, Illinois 60607, United States;* orcid.org/0000-0001-7398-8521

Tom G. Driver − *Department of Chemistry, University of Illinois Chicago, Chicago, Illinois 60607, United States;* orcid.org/0000-0001-7001-342X

Complete contact information is available at: https://pubs.acs.org/10.1021/acs.jpca.5c02567

Author Contributions

N.G. and K.G. conceived the research and designed the research approach. K.G., T.G.D., and R.J.H. acquired the funding for this project. H.Z. synthesized the model compounds. J.M.O. and N.G. collected the femtosecond transient absorption spectroscopy data. N.G. performed the experiments, collected, and analyzed the raw data. K.G. provided supervision. N.G. wrote the initial manuscript with input from K.G. All authors contributed to the writing of the final version of the manuscript.

Funding

Extreme Energy Density (EXEED), an Army HBCU/MI Center of Excellence at the University of Illinois Chicago, under Grant No. W911NF2110275 from the Army Research Office and U.S. Department of Energy-National Nuclear Security Administration (DOE-NNSA) Cooperative Agreement No. DE-NA-0004153 (Chicago/DOE Alliance Center, CDAC).

Notes

The authors declare no competing financial interest.

■ ACKNOWLEDGMENTS

N.G., H.Z., R.J.H., T.G.D., and K.G. gratefully acknowledge Extreme Energy Density (EXEED), an Army HBCU/MI Center of Excellence at the University of Illinois Chicago, under Grant No. W911NF2110275 from the Army Research Office, and the U.S. Department of Energy-National Nuclear Security Administration (DOE-NNSA) Cooperative Agreement No. DE-NA-0004153 (Chicago/DOE Alliance Center, CDAC) for funding this work. We thank H.Z. and T.G.D. for synthesizing the three model compounds for this study. We also thank J.M.O. and A.J.A. for collecting femtosecond transient absorption spectroscopy data. We thank the Laboratory Computing Resources Center (LCRC) at Argonne National Laboratory (ANL) for providing the advanced computing resources used for DFT calculations.

■ ABBREVIATIONS

RO, ring opening; TD_{24}, temperature at which the maximum decomposition rate is 24 h; DFT, density functional theory; IEFPCM, integral equation formalism polarizable continuum mode; TD-DFT, time-dependent density functional theory

■ REFERENCES

(1) Driver, T. G. Recent Advances in Transition Metal-Catalyzed N-Atom Transfer Reactions of Azides. *Org. Biomol. Chem.* **2010**, *8* (17), 3831.

(2) Schock, M.; Bräse, S. Reactive & Efficient: Organic Azides as Cross-Linkers in Material Sciences. *Molecules* **2020**, *25* (4), 1009.

(3) Bräse, S.; Gil, C.; Knepper, K.; Zimmermann, V. Organic Azides: An Exploding Diversity of a Unique Class of Compounds. *Angew. Chem. Int. Ed.* **2005**, *44* (33), 5188−5240.

(4) Nyffeler, P. T.; Liang, C.-H.; Koeller, K. M.; Wong, C.-H. The Chemistry of Amine−Azide Interconversion: Catalytic Diazotransfer and Regioselective Azide Reduction. *J. Am. Chem. Soc.* **2002**, *124* (36), 10773−10778.

(5) Lang, S.; Murphy, J. A. Azide Rearrangements in Electron-Deficient Systems. *Chem. Soc. Rev.* **2006**, *35* (2), 146−156.

(6) Wang, C.; Ikhlef, D.; Kahlal, S.; Saillard, J.-Y.; Astruc, D. Metal-Catalyzed Azide-Alkyne "Click" Reactions: Mechanistic Overview and Recent Trends. *Coord. Chem. Rev.* **2016**, *316*, 1−20.

(7) Huisgen, R.; Knorr, R.; Möbius, L.; Szeimies, G. 1.3-Dipolare Cycloadditionen, XXIII. Einige Beobachtungen Zur Addition Organischer Azide an CC-Dreifachbindungen. *Chem. Ber.* **1965**, *98* (12), 4014−4021.

(8) Stanovnik, B. Application of Organic Azides in the Synthesis of Heterocyclic Systems. *Advances in Heterocyclic Chemistry*; Elsevier, 2020, Vol. *130*, pp. 145−194. DOI:.

(9) Xie, S.; Sundhoro, M.; Houk, K. N.; Yan, M. Electrophilic Azides for Materials Synthesis and Chemical Biology. *Acc. Chem. Res.* **2020**, *53* (4), 937−948.

(10) Meng, G.; Guo, T.; Ma, T.; Zhang, J.; Shen, Y.; Sharpless, K. B.; Dong, J. Modular Click Chemistry Libraries for Functional Screens Using a Diazotizing Reagent. *Nature* **2019**, *574* (7776), 86−89.

(11) Soni, J. P.; Kadagathur, M.; Shankaraiah, N. Recent Updates on Azido-reductive Cyclization Approaches: Syntheses of *Aza* -Heterocyclic Frameworks. *Asian J. Org. Chem.* **2021**, *10* (12), 3186−3200.

(12) Swenton, J. S.; Ikeler, T. J.; Williams, B. H. Photochemistry of Singlet and Triplet Azide Excited States. *J. Am. Chem. Soc.* **1970**, *92* (10), 3103−3109.

(13) Gritsan, N.; Platz, M. Photochemistry of Azides: The Azide/Nitrene Interface. In *Organic Azides*; Wiley, 2009, pp. 311−372. .

(14) Ju, M.; Schomaker, J. M. Nitrene Transfer Catalysts for Enantioselective C−N Bond Formation. *Nat. Rev. Chem.* **2021**, *5* (8), 580−594.

(15) Osisioma, O.; Patton, L. J.; Merugu, R.; Govorov, D.; Milbrandt, M. A.; Jarus, C.; Karney, W. L.; Gudmundsdottir, A. D. Formation of Stilbene Azo-Dimer by Direct Irradiation of P-Azidostilbene †. *Photochem. Photobiol.* **2023**, *99* (2), 605−615.

(16) Kolb, H. C.; Sharpless, K. B. The Growing Impact of Click Chemistry on Drug Discovery. *Drug Discov. Today* **2003**, *8* (24), 1128−1137.

(17) Breinbauer, R.; Köhn, M. Azide−Alkyne Coupling: A Powerful Reaction for Bioconjugate Chemistry. *ChemBiochem* **2003**, *4* (11), 1147−1149.

(18) Abu Bakar, R.; Li, Y.; Hewitson, O. P.; Roth, P. J.; Keddie, J. L. Azide Photochemistry in Acrylic Copolymers for Ultraviolet Cross-Linkable Pressure-Sensitive Adhesives: Optimization, Debonding-on-Demand, and Chemical Modification. *ACS Appl. Mater. Interfaces* **2022**, *14* (26), 30216−30227.

(19) Krasutsky, A. P.; Kuehl, C. J.; Zhdankin, V. V. Direct Azidation of Adamantane and Norbornane by Stable Azidoiodinanes. *Synlett* **1995**, *1995* (10), 1081−1082.

(20) Zhdankin, V. V.; Krasutsky, A. P.; Kuehl, C. J.; Simonsen, A. J.; Woodward, J. K.; Mismash, B.; Bolz, J. T. Preparation, X-Ray Crystal Structure, and Chemistry of Stable AzidoiodinanesDerivatives of Benziodoxole. *J. Am. Chem. Soc.* **1996**, *118* (22), 5192−5197.

(21) Zhdankin, V. V.; Kuehl, C. J.; Krasutsky, A. P.; Formaneck, M. S.; Bolz, J. T. Preparation and Chemistry of Stable Azidoiodinanes: 1-Azido-3,3-Bis(Trifluoromethyl)-3-(1H)-1,2-Benziodoxol and 1-Azido-1,2-Benziodoxol-3-(1H)-One. *Tetrahedron Lett.* **1994**, *35* (52), 9677−9680.

(22) Mironova, I. A.; Kirsch, S. F.; Zhdankin, V. V.; Yoshimura, A.; Yusubov, M. S. Hypervalent Iodine-Mediated Azidation Reactions. *Eur. J. Org. Chem.* **2022**, *2022* (34), No. e202200754.

(23) Wang, X.; Studer, A. Iodine(III) Reagents in Radical Chemistry. *Acc. Chem. Res.* **2017**, *50* (7), 1712−1724.

(24) Stang, P. J.; Zhdankin, V. V. Organic Polyvalent Iodine Compounds. *Chem. Rev.* **1996**, *96*, 1123−1178.
(25) Martin, J. C. "Frozen" Transition States: Pentavalent Carbon Et Al. *Science* **1983**, *221* (4610), 509−514.
(26) Kiyokawa, K.; Nakano, K.; Okumatsu, D.; Minakata, S. Photoinduced Azidoamination of Styrenes Using Sodium Azide and (Diphenylmethylene)Amino Benziodoxolone. *Chem. -Asian J.* **2025**, *20*, No. e202401493.
(27) Lu, Z.; Putziger, J.; Lin, S. Light-Activated Hypervalent Iodine Agents Enable Diverse Aliphatic C−H Functionalization. *Nat. Chem.* **2025**, *17*, 365.
(28) Yang, J.; Li, M.; Xue, X. Computational I(III)—X BDEs for Benziodoxol(on)E-based Hypervalent Iodine Reagents: Implications for Their Functional Group Transfer Abilities. *Chin. J. Chem.* **2019**, *37* (4), 359−363.
(29) Wu, D.; Cui, S.-S.; Lin, Y.; Li, L.; Yu, W. Visible Light-Driven Azidation/Difunctionalization of Vinyl Arenes with Azidobenziodoxole under Copper Catalysis. *J. Org. Chem.* **2019**, *84* (17), 10978−10989.
(30) Cong, F.; Wei, Y.; Tang, P. Combining Photoredox and Silver Catalysis for Azidotrifluoromethoxylation of Styrenes. *Chem. Commun.* **2018**, *54* (35), 4473−4476.
(31) Rabet, P. T. G.; Fumagalli, G.; Boyd, S.; Greaney, M. F. Benzylic C−H Azidation Using the Zhdankin Reagent and a Copper Photoredox Catalyst. *Org. Lett.* **2016**, *18* (7), 1646−1649.
(32) Alazet, S.; Preindl, J.; Simonet-Davin, R.; Nicolai, S.; Nanchen, A.; Meyer, T.; Waser, J. Cyclic Hypervalent Iodine Reagents for Azidation: Safer Reagents and Photoredox-Catalyzed Ring Expansion. *J. Org. Chem.* **2018**, *83* (19), 12334−12356.
(33) Fumagalli, G.; Rabet, P. T. G.; Boyd, S.; Greaney, M. F. Three-Component Azidation of Styrene-Type Double Bonds: Light-Switchable Behavior of a Copper Photoredox Catalyst. *Angew. Chem. Int. Ed.* **2015**, *54* (39), 11481−11484.
(34) Wang, Y.; Hu, X.; Morales-Rivera, C. A.; Li, G.-X.; Huang, X.; He, G.; Liu, P.; Chen, G. Epimerization of Tertiary Carbon Centers via Reversible Radical Cleavage of Unactivated C(Sp 3)−H Bonds. *J. Am. Chem. Soc.* **2018**, *140* (30), 9678−9684.
(35) Fuentes, N.; Kong, W.; Fernández-Sánchez, L.; Merino, E.; Nevado, C. Cyclization Cascades via *N* -Amidyl Radicals toward Highly Functionalized Heterocyclic Scaffolds. *J. Am. Chem. Soc.* **2015**, *137* (2), 964−973.
(36) Kong, W.; Fuentes, N.; García-Domínguez, A.; Merino, E.; Nevado, C. Stereoselective Synthesis of Highly Functionalized Indanes and Dibenzocycloheptadienes through Complex Radical Cascade Reactions. *Angew. Chem., Int. Ed.* **2015**, *127* (8), 2517−2521.
(37) Shirke, R. P.; Ramasastry, S. S. V. Organocatalytic β-Azidation of Enones Initiated by an Electron-Donor−Acceptor Complex. *Org. Lett.* **2017**, *19* (19), 5482−5485.
(38) Lonca, G. H.; Ong, D. Y.; Tran, T. M. H.; Tejo, C.; Chiba, S.; Gagosz, F. Anti-Markovnikov Hydrofunctionalization of Alkenes: Use of a Benzyl Group as a Traceless Redox-Active Hydrogen Donor. *Angew. Chem. Int. Ed.* **2017**, *56* (38), 11440−11444.
(39) Chen, L.; Xing, H.; Zhang, H.; Jiang, Z.-X.; Yang, Z. Copper-Catalyzed Intermolecular Chloroazidation of α,β-Unsaturated Amides. *Org. Biomol. Chem.* **2016**, *14* (31), 7463−7467.
(40) Yu, L.-Z.; Wei, Y.; Shi, M. Copper-Catalyzed Cascade Cyclization of 1,5-Enynes via Consecutive Trifluoromethylazidation/Diazidation and Click Reaction: Self-Assembly of Triazole Fused Isoindolines. *Chem. Commun.* **2016**, *52* (89), 13163−13166.
(41) Ouyang, X.-H.; Song, R.-J.; Liu, Y.; Hu, M.; Li, J.-H. Copper-Catalyzed Radical [2 + 2 + 1] Annulation of Benzene-Linked 1, *n* -Enynes with Azide: Fused Pyrroline Compounds. *Org. Lett.* **2015**, *17* (24), 6038−6041.
(42) Day, C. S.; Fawcett, A.; Chatterjee, R.; Hartwig, J. F. Mechanistic Investigation of the Iron-Catalyzed Azidation of Alkyl C(*Sp* 3)−H Bonds with Zhdankin's λ 3 -Azidoiodane. *J. Am. Chem. Soc.* **2021**, *143* (39), 16184−16196.
(43) Kirschning, A.; Hashem, M.; Monenschein, A.; Rose, H.; Schöning, L. K.-U. Preparation of Novel Haloazide Equivalents by Iodine(III)-Promoted Oxidation of Halide Anions. *J. Org. Chem.* **1999**, *64* (17), 6522−6526.
(44) Leyva, E.; Platz, M. S.; Loredo-Carrillo, S. E.; Aguilar, J. Fluoro Aryl Azides: Synthesis, Reactions and Applications. *Curr. Org. Chem.* **2020**, *24* (11), 1161−1180.
(45) Matsumoto, K.; Nakajima, M.; Nemoto, T. Determination of the Best Functional and Basis Sets for Optimization of the Structure of Hypervalent Iodines and Calculation of Their First and Second Bond Dissociation Enthalpies. *J. Phys. Org. Chem.* **2019**, *32* (8), No. e3961.
(46) Andris, E.; Navrátil, R.; Jašík, J.; Sabenya, G.; Costas, M.; Srnec, M.; Roithová, J. Spin-State-Controlled Photodissociation of Iron(III) Azide to an Iron(V) Nitride Complex. *Angew. Chem. Int. Ed.* **2017**, *56* (45), 14057−14060.
(47) Torres-Alacan, J.; Krahe, O.; Filippou, A. C.; Neese, F.; Schwarzer, D.; Vöhringer, P. The Photochemistry of [Fe III N 3 (Cyclam-ac)]PF 6 at 266lNm. *Chem. - Eur. J.* **2012**, *18* (10), 3043−3055.
(48) Gonzalez, M. C.; Le Roux, G. C.; Rosso, J. A.; Braun, A. M. Mineralization of CCl4 by the UVC-Photolysis of Hydrogen Peroxide in the Presence of Methanol. *Chemosphere* **2007**, *69* (8), 1238−1244.
(49) Zhu, C.; Yu, Y.; Pan, X.; Dong, W.; Hou, H. UV Photolysis Mechanism of CCl4 and CHCl3 in Water. *Huan Jing Ke Xue.* **2001**, *22* (3), 6−10.
(50) Kobayashi, Y.; Chang, K. F.; Zeng, T.; Neumark, D. M.; Leone, S. R. Direct Mapping of Curve-Crossing Dynamics in IBr by Attosecond Transient Absorption Spectroscopy. *SCIENCE* **2019**, *365*, 79−83.
(51) Garwood, J. J. A.; Chen, A. D.; Nagib, D. A. Radical Polarity. *J. Am. Chem. Soc.* **2024**, *146*, 28034−28059.
(52) De Vleeschouwer, F.; Van Speybroeck, V.; Waroquier, M.; Geerlings, P.; De Proft, F. Electrophilicity and Nucleophilicity Index for Radicals. *Org. Lett.* **2007**, *9* (14), 2721−2724.
(53) Parsaee, F.; Senarathna, M. C.; Kannangara, P. B.; Alexander, S. N.; Arche, P. D. E.; Welin, E. R. Radical Philicity and Its Role in Selective Organic Transformations. *Nat. Rev. Chem.* **2021**, *5* (7), 486−499.
(54) Roberts, B. P. Polarity-Reversal Catalysis of Hydrogen-Atom Abstraction Reactions: Concepts and Applications in Organic Chemistry. *Chem. Soc. Rev.* **1999**, *28* (1), 25−35.
(55) Elliot, A. J. A Pulse Radiolysis Study of the Reaction of OH with I 2 and the Decay of I $_2$ −. *Can. J. Chem.* **1992**, *70* (6), 1658−1661.
(56) Gardner, J. M.; Abrahamsson, M.; Farnum, B. H.; Meyer, G. J. Visible Light Generation of Iodine Atoms and I−I Bonds: Sensitized I − Oxidation and I 3 − Photodissociation. *J. Am. Chem. Soc.* **2009**, *131* (44), 16206−16214.
(57) Mezyk, S. P. Rate Constant and Arrhenius Parameter Determination for the Reaction of the Hydrated Electron with Iodomethane, Iodoethane, 1-Iodopropane and 2-Iodopropane in Aqueous Solution. *Radiat. Phys. Chem.* **1997**, *49* (4), 437−443.

https://doi.org/10.1021/acs.jpca.5c02567
J. Phys. Chem. A XXXX, XXX, XXX−XXX